Observation and Control of Laser-Enabled Auger Decay

D. Iablonskyi,[1] K. Ueda,[1,*] K. L. Ishikawa,[2,3] A. S. Kheifets,[4] P. Carpeggiani,[5] M. Reduzzi,[5] H. Ahmadi,[5] A. Comby,[5] G. Sansone,[5,6] T. Csizmadia,[7] S. Kuehn,[7] E. Ovcharenko,[8] T. Mazza,[8] M. Meyer,[8] A. Fischer,[9] C. Callegari,[10] O. Plekan,[10] P. Finetti,[10] E. Allaria,[10] E. Ferrari,[10] E. Roussel,[10] D. Gauthier,[10] L. Giannessi,[10,11] and K. C. Prince[10,12,†]

[1]*Institute of Multidisciplinary Research for Advanced Materials, Tohoku University, Sendai 980-8577, Japan*
[2]*Department of Nuclear Engineering and Management, Graduate School of Engineering, The University of Tokyo, 7-3-1 Hongo, Bunkyo-ku, Tokyo 113-8656, Japan*
[3]*Photon Science Center, Graduate School of Engineering, The University of Tokyo, 7-3-1 Hongo, Bunkyo-ku, Tokyo 113-8656, Japan*
[4]*Research School of Physics and Engineering, Australian National University, Canberra, ACT 2601, Australia*
[5]*Dipartimento di Fisica, CNR-IFN, Politecnico di Milano, 20133 Milan, Italy*
[6]*Physikalisches Institut der Albert-Ludwigs-Universitat, 79104 Freiburg, Germany*
[7]*ELI-ALPS, Pintér József utca, 6728 Szeged, Hungary*
[8]*European XFEL GmbH, 22869 Schenefeld, Germany*
[9]*Max Planck Institute for Nuclear Physics, Heidelberg 69117, Germany*
[10]*Elettra-Sincrotrone Trieste, 34149 Basovizza, Trieste, Italy*
[11]*ENEA C.R. Frascati, 00044 Frascati, Rome, Italy*
[12]*Molecular Model Discovery Laboratory, Department of Chemistry and Biotechnology, Swinburne University of Technology, Melbourne 3122, Australia*

(Received 4 May 2017; published 14 August 2017)

Single-photon laser-enabled Auger decay (spLEAD) is predicted theoretically [B. Cooper and V. Averbukh, Phys. Rev. Lett. **111**, 083004 (2013)] and here we report its first experimental observation in neon. Using coherent, bichromatic free-electron laser pulses, we detect the process and coherently control the angular distribution of the emitted electrons by varying the phase difference between the two laser fields. Since spLEAD is highly sensitive to electron correlation, this is a promising method for probing both correlation and ultrafast hole migration in more complex systems.

DOI: 10.1103/PhysRevLett.119.073203

When isolated atoms or molecules are excited, they relax to their ground state in two ways: via nuclear motion or electronically. Two possible ways of releasing electronic energy are by radiation and by Auger decay. The Auger process [1,2] first reported by Meitner, has played an important part in modern physics, particularly surface science, because it is by far the strongest decay channel for core holes of light elements such as carbon, nitrogen, and oxygen. However, for the ionization of some inner valence levels of atoms and molecules, the Auger process is energetically forbidden, because the energy of the doubly ionized final state is higher than the energy of the initial ion. In this case, new electronic mechanisms for deexcitation may be discovered that depend on the environment of the ionized state.

It was predicted some time ago that such states could decay by the novel process of interatomic or intermolecular Coulombic decay (ICD) [3], if the excited or ionized species was weakly bound to its environment. In this process, the final state of the system contains two positive charges, but the charge is distributed between the original atom or molecule and its neighbor, thus lowering the energy because the Coulomb repulsion between the charges is reduced. This prediction led subsequently to intense research activity, with many new discoveries reported, as it was found that ICD and its variants could occur in many different ways [4–9].

Another electronic decay process that has been theoretically predicted is single-photon laser-enabled Auger decay (spLEAD) [10], in which the extra energy required to reach the doubly ionized state is supplied by a single photon. In the absence of correlation, this process is forbidden, but it becomes allowed due to correlation. While the single-photon process has not yet been observed, multiphoton laser-enabled Auger decay (LEAD), which is an allowed process, has been observed. LEAD was observed for $3s$ ionized argon (and for other inner valence ionized noble gases), which normally decay by fluorescence [11,12]. In the presence of a strong infrared field, the ion can absorb multiple photons and decay to a doubly $3p$ ionized state. This method has been used to coherently control the yield of singly and doubly ionized atoms in two-color experiments [13]. With this technique, only the phase of the infrared light with respect to the envelope of the short wavelength light is important, and the phase of the short wavelength light is not relevant: oscillations as a function

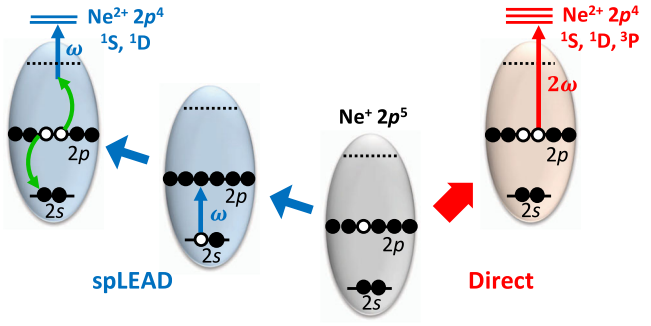

FIG. 1. Schematic diagram for the ionization of Ne $2s^2 2p^5$. Center: initial state. Left (blue arrows): (1) the spLEAD process follows (2) absorption of one ω photon. Right (red arrows): direct ionization by 2ω, process (3).

of phase occur with the period (or half period) of the IR light, about 2.6 (1.3) fs. Like ICD, LEAD and spLEAD are new decay modes of excited states, and both mechanisms depend on the environment of the atom or molecule: in one case, neighboring neutral atoms or molecules, and in the second case, the surrounding photon field.

In the present Letter, we report the observation of spLEAD and we describe a different kind of coherent control of the process, in which the phase difference between two wavelengths is controlled. We manipulate the angular distribution of the emitted Auger electrons using the relative phase of the ionizing and enabling laser beams. Because spLEAD relies on electron correlations, it can potentially provide novel information such as correlation-induced ultrafast hole migration in molecules [10,14–18].

The processes studied are illustrated graphically in Fig. 1 for the neon atom. The spLEAD takes place for the 2s-hole state in Ne^+:

$$2s^1 2p^6 + \omega \rightarrow 2s^2 2p^4 (^1S, ^1D) + e. \quad (1)$$

Within LS coupling, only the ^1S and ^1D final states are allowed in spLEAD even though the $2s^2 2p^4$ configuration can, in principle, couple into the ^3P term. This is because the intermediate $2s^1 2p^6$ configuration is in the S state. As mentioned, spLEAD is made allowed by configuration mixing [10] and the configurations that can mix with the pure $2s^1 2p^6$ configuration are those such as $2s^2 2p^4 (^1D_2) 3d\ S_{1/2}$, $2s^2 2p^4 (^1S_0) 3s\ S_{1/2}$, etc. These configurations consist of a ^1S or ^1D core and a d or s electron, which can be thought of conceptually as the Auger electron.

We do not prepare the 2s-hole state directly, but begin from an initial state consisting of $2s^2 2p^5\ ^2P_{1/2}$ ions. These are created by the ionization of neutral Ne by either ω or 2ω, and then converted to 2s-hole states by absorption of a single photon:

$$2s^2 2p^5 + \omega \rightarrow 2s^1 2p^6, \quad (2)$$

where $\omega = 26.91$ eV is tuned to the energy difference between $2s^2 2p^5$ and $2s^1 2p^6$. In addition, we simultaneously ionize the ground state $2s^2 2p^5$ of Ne^+ by the phase-locked second harmonic 2ω (53.82 eV) to access all of the ^1S, ^1D, and ^3P final states of Ne^{2+} (Fig. 1, right):

$$2s^2 2p^5 + 2\omega \rightarrow 2s^2 2p^4 (^1S, ^1D, ^3P) + e^-. \quad (3)$$

The $2s^2 2p^5$ ionic states can be directly ionized by process (3), or indirectly by processes (2) and (1) (Fig. 1, left):

$$2s^2 2p^5 + \omega + \omega \rightarrow 2s^1 2p^6 + \omega \rightarrow 2s^2 2p^4 (^1S, ^1D) + e^-. \quad (4)$$

The key point is that the two light pulses ω and 2ω are phase coherent. As a result, the two paths (3) and (4) to the same final states ^1S and ^1D interfere, but only path (3) leads to ^3P, so no interference occurs.

To investigate the spLEAD process exhibited in Fig. 1, we chose to use the recently demonstrated capability of the FERMI light source to produce intense bichromatic radiation with a controllable phase [19]. This free electron laser (FEL) produces pulses of light with commensurate wavelengths (such as the first and second harmonics used here), and that are naturally locked in phase. The phase can be controlled by manipulating the electron beam path, resulting in a phase resolution corresponding to a few attoseconds. We provided conditions in which there are two quantum paths to a photoelectron state with a defined linear momentum, and we coherently controlled these quantum paths. With this approach, we observed a signal proportional to the amplitude, rather than the intensity, of the quantum processes. As we will see below, the signals we detect are of the order 2%. Since they are proportional to the square root of the coupling constant, $\sqrt{c}$, we expect other signals such as the change in total ionization, proportional to c, to be of the order 0.05%, too small to detect. The approach of measuring a signal proportional to the phase brings considerable advantages when detecting a weak signal with a strong background [20].

We illustrate here how the spLEAD emission can be coherently controlled and detected in the photoelectron angular distribution (PAD), using that of the ^1S final state as an example. Process (4) emits a p wave electron while process (3) is assumed to emit mainly a d wave electron, by the Fano propensity rule [21]. The angular distribution can then be written as

$$I(\theta, \phi) \propto |Y_{20}(\theta, \phi) e^{i\eta} + \sqrt{c} Y_{10}(\theta, \phi) e^{i\delta_{PD}}|^2, \quad (5)$$

where $Y_{nl}(\theta, \phi)$ denote spherical harmonics, and the coupling constant $c(\ll 1)$ is proportional to the intensity of the spLEAD path (4) relative to the direct photoionization (3), and therefore is also proportional to the intensities of the two colors. δ_{PD} is the phase difference of the outgoing waves (described by spherical harmonics), and η is the $\omega - 2\omega$ relative phase. Note that the relative intensity enters the equation as the term $\sqrt{c}$, that is, as the relative amplitudes of the two coherent beams. Then, the asymmetry of the electron emission, defined as the

difference between the emission in one hemisphere ($0 < \theta < \pi/2$) and the other ($\pi/2 < \theta < \pi$), divided by the sum, is expressed as

$$A(\eta) = \frac{\sqrt{15}}{4}\frac{\sqrt{c}}{1+c}\cos(\eta - \delta_{\mathrm{PD}}). \quad (6)$$

This oscillates as a function of the relative phase η between the two harmonics, and its amplitude is approximately $\sqrt{c}(\gg c)$ instead of c.

The experiment was performed at the low density matter beam line [22] of FERMI. The sample consisted of a mixture of neon and helium (for calibration purposes) and was exposed to a bichromatic beam of temporally overlapping first and second harmonic radiation with a controlled phase relationship [19]. In the present experiment, the FEL fundamental wavelength was generated by tuning the sixth undulator of the radiator to the fifth harmonic of the seed wavelength (230.4 nm). The second harmonic of the FEL was generated by tuning the first five undulators to the tenth harmonic of the seed, giving rise to bichromatic phase-locked pulses. The photon energies were $\omega = 26.91$ eV and $2\omega = 53.82$ eV, where ω, as stated, was equal to the difference in energy between the $2s^2 2p^5$ and $2s^1 2p^6$ Ne^+ ionic states (see Fig. 1). The light was focused to a spot size of approximately 5 μm FWHM. The calculated pulse durations were 75 fs for the first and 60 fs for the second harmonic.

Under the above conditions, the kinetic energies of the photoelectrons emitted by the fundamental $\omega = 26.91$ eV (from the $2p$ subshell) and by the second harmonic $2\omega = 53.82$ eV (from the $2s$ subshell) are identical. Furthermore, similar ionization rates of $2p$ by the fundamental (ω) and 2s by the second harmonic (2ω) were set. Single ionization generates our sample, which is a mixture of $2s^2 2p^5$ and $2s^1 2p^6$ Ne^+ ions formed by three different processes: $2p$ ionization by ω

$$2s^2 2p^6 + \omega \rightarrow 2s^2 2p^5 + e^-, \quad (7)$$

$2p$ ionization by 2ω

$$2s^2 2p^6 + 2\omega \rightarrow 2s^2 2p^5 + e^-, \quad (8)$$

and $2s$ ionization by 2ω

$$2s^2 2p^6 + 2\omega \rightarrow 2s^1 2p^6 + e^-. \quad (9)$$

These ionic states, which are our target initial states of processes (1)–(4), are independent and have no quantum phase relationship.

The Ne-He mixture was introduced into the experimental chamber using a pulsed valve (Parker model 9, convergent-to-cylindrical nozzle with a cylindrical aperture of 250 μm diameter) at room temperature. Helium was added as a calibrant and as a cross-check for spurious artifacts. The electron spectra were measured using a velocity map imaging spectrometer, and the spectra were reconstructed from the raw data using the pBASEX algorithm [23].

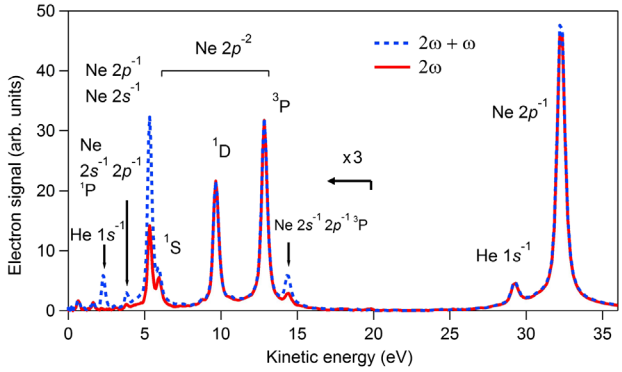

FIG. 2. Electron kinetic energy spectra of atomic Ne irradiated by $\omega = 26.91$ eV and $2\omega = 53.82$ eV (dashed blue curve) and 2ω only (continuous red curve).

The spectrum (at a fixed relative phase) is shown in Fig. 2, together with the line assignments. Several features are present in the spectrum, of which the most prominent are the single-photon emission of $2p$ and $2s$ electrons from neutral Ne at 5.3 eV (by ω and 2ω, respectively; the photoelectrons have the same kinetic energy), single photon ionization of $2p$ by 2ω (32.2 eV), and emission corresponding to doubly ionized Ne^{2+} final states ^1S, ^1D, and ^3P.

In principle, spLEAD may be observed directly as an increase in the photoelectron yield of the ^1S and ^1D final states when the ω field is applied, Eq. (4). However, the increase (estimated above to be ~0.04% in the present case) is too small to be detected above the noise. Indeed, within experimental error, the intensities of the ^1S and ^1D peaks in Fig. 2 did not change when the first harmonic was added. In the PAD, however, we observed an oscillation of the asymmetry $A(\eta)$ as a function of the phase difference between the harmonics, see Fig. 3. Note that the zero of the relative phase is not absolute, but has an arbitrary offset. We observe strong modulation of the $2p^4$ ^1S and ^1D states as a function of the phase, while the ^3P state shows much weaker or negligible modulation. The helium and neon single ionization peaks show no effect, as expected. The oscillation in the PADs indicates that indeed the final states can be reached from an initial state by more than one pathway, and that these pathways are coherent.

We note that our measurement belongs to the Brumer-Shapiro class of bichromatic experiments. In such experiments, the phase-locked first and second harmonics create two quantum paths for the emission of a photoelectron of given momentum, causing interference [24], for example, by single-photon and two-photon ionization of the same electron state. The conditions we have chosen also set up interference, but in a quite different way from the usual Brumer-Shapiro approach, where single-photon and two-photon processes interfere. Here, the interference appears as a phase-dependent asymmetry of the PADs as given by Eq. (6).

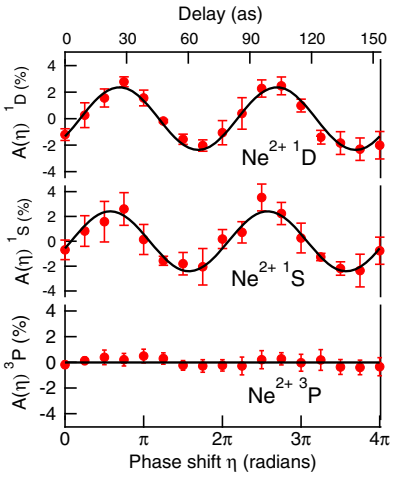

FIG. 3. Asymmetry $A(\eta)$ of photoelectron angular distributions corresponding to the final ionic states ^1S, ^1D, and ^3P of Ne^{2+}, as a function of the phase shift between the first and second harmonic. The asymmetry $A(\eta)$ is defined as the difference between the emission in one hemisphere ($0 < \theta < \pi/2$) and the other ($\pi/2 < \theta < \pi$), divided by the sum of the emission.

In order to confirm that the observed oscillations stem from coherently controlled spLEAD, we estimate the amplitudes for the oscillation of $A(\eta)$ in Fig. 3. We use the experimental conditions captured in the photoelectron spectra in Fig. 2, and the calculated spLEAD cross section. From the spectrum in which only the second harmonic was present (solid red curve in Fig. 2), we extract the intensities of the photoelectron peaks corresponding to processes (3), (8), and (9), as well as the following process:

$$2s^1 2p^6 + 2\omega \rightarrow 2s^1 2p^5 (^{1,3}P) + e^- \qquad (10)$$

with electron kinetic energies of 3.85 eV (^1P) and 14.4 eV (^3P). In ion spectra (data not shown), the ratio of $Ne^+ : Ne^{2+}$ was found to be 3.85. This was combined with the known photoionization cross sections [6.7, 6.8, and 0.3 Mb for processes (3), (8), and (9), respectively [25,26], and the calculated cross section of 6.8 Mb for process (10)], to give an estimate of the intensity of 2ω of 2.0×10^{13} W/cm^2. This was done by solving the rate equations and taking account of the pulse duration and the spot size given above; Gaussian temporal and spatial profiles were used. From the spectrum (dashed blue curve in Fig. 2), where the fundamental radiation ω was added without altering the intensity of 2ω, we again extract photoelectron intensities including that for process (7). From the intensity ratios of photoelectrons of processes (7)–(9) and known cross sections for these processes [8.4 Mb for process (7), [26]], we estimate the intensity ratio between ω and 2ω to be 1 : 52, and, hence, the intensity of ω to be 3.8×10^{11} W/cm^2.

Furthermore, as can be seen in Fig. 2, the addition of ω leads to a significant enhancement of the overlapping peak of $2p$ and $2s$ photoelectrons for processes (7) and (9), respectively, and of the intensity for process (10). These observations clearly demonstrate that the fundamental radiation ω indeed enhances the population of $2s^1 2p^6$ via the $2s$-$2p$ hole coupling (2). From the magnitude of the enhancement of the photoelectron peak arising from process (10), relative to the photoelectron peak intensities of processes (7) and (8), we estimate the effective probability of process (2) to be 0.065.

As stated above, the amplitude for the oscillation of $A(\eta)$ in Eq. (6) is equal to the amplitude of the spLEAD process (4) relative to the direct ionization process (2), i.e., $\approx\sqrt{c}$ in Eq. (5); both follow practically the same first step ionization dominated by process (8). The only missing parameter needed to estimate $\sqrt{c}$ is therefore the amplitude of the spLEAD process (1). The estimate of $\sqrt{c}$ employing the spLEAD cross section reported in the literature [10], however, resulted in $\sqrt{c} \approx 0.001$, roughly 1 order smaller than the present observation $\sqrt{c} \approx 0.02$. Our own calculations including only the static correlations (i.e., configuration mixing in $2s^1 2p^6\ ^2S_{1/2}$) are in good agreement with the literature value. We thus extended the calculations to include the dynamic correlations (continuum-continuum coupling) using the following expression:

$$M(\nu_f, \nu_0; l_n) = \left\{ \sum_{\varepsilon_{\nu_n}<0} + \int_0^\infty d\varepsilon_{\nu_n} \right\} \frac{d_{\nu_f \nu_n}(\omega) D_{\nu_n \nu_0}}{\omega_{n0} - \omega - i\delta}. \qquad (11)$$

Here, ν_0 is the initial $2s$ state, ν_n is an intermediate state $2p^4 n\ell$ or $2p^4 \varepsilon\ell$, $\ell = 0, 2$, and ν_f is the ϵp or f final state; ω_{n0} is the energy difference between the intermediate and initial state. The Auger decay matrix element $D_{\nu_n \nu_0}(\omega_j)$ is calculated using the computer code described in Ref. [27]. The discrete sum in this equation is equivalent to inclusion of the static correlation in Ref. [10]. The dipole matrix elements $d_{\nu_f \nu_n}$ for the continuum-continuum transitions are singular. Their integration is handled using the numerical recipe of Ref. [28].

The oscillation amplitudes calculated using these estimates are 0.82% for the ^1S peak and 1.4% for ^1D, in rough agreement with our observation, $2.40\% \pm 0.34\%$ for ^1S and $2.33\% \pm 0.18\%$ for ^1D. Coupling of $2s^1 2p^6$ (^1S) to the lowest discrete states $2s^2 2p^4 (^1S) ns$ is stronger than to $2s^2 2p^4 (^1D) nd$ as can be seen from the corresponding spectroscopic factors [29]. However, this propensity is lost for higher excited states and especially the continuum states where the ^1S and ^1D continua have about the same strength, as observed experimentally. The discrepancy between the theoretical and experimental values may stem from the experimental uncertainties and theoretical approximations involved. Note that here, unlike in Eqs. (5) and (6), more exact treatments, with the inclusion of the weaker s wave for process (3) and taking account of the ^1D final state, are used. The observed oscillations of the ^1S and ^1D asymmetry show a phase offset of 0.36 ± 0.14 rad, in qualitative agreement with the predictions of theory, but significantly smaller than the calculated value of 1.27 rad. The discrepancy is most likely due to the limits of the accuracy with

which the phase offset and matrix elements can be calculated.

In summary, we have shown how the technique of coherent control can be applied to observe a new phenomenon, spLEAD, which for the present case of neon is too weak to be observed directly as an intensity enhancement. We detected the process by using a method that depends on amplitude rather than intensity. Furthermore, we manipulated the outcome of the ionization process, in terms of the emission direction of the photoelectrons. Cooper and Averbukh [10] calculated that oxygen 2*s* holes of glycine have a far higher cross section for spLEAD, implying that detection is much easier. Our results suggest that spLEAD may be observable as an increase in cross section for molecules containing oxygen, which includes many biomolecules. Noting that the sudden creation of the O 2*s* hole causes ultrafast charge dynamics, our work shows the way to investigating charge dynamics not only by the pump-probe methods proposed by Cooper and Averbukh [10], but also by the sophisticated methods of coherent control. The complex and ultrafast dynamics of inner-valence hole wave packets, or electron correlations, may now be investigated and coherently controlled by using the coherence of bichromatic light with a resolution of a few attoseconds.

This work was supported in part by the X-ray Free Electron Laser Utilization Research Project and the X-ray Free Electron Laser Priority Strategy Program of the Ministry of Education, Culture, Sports, Science, and Technology of Japan (MEXT) and the IMRAM program of Tohoku University, and the Dynamic Alliance for Open Innovation Bridging Human, Environment and Materials program. K. L. I. gratefully acknowledges support by the Cooperative Research Program of the "Network Joint Research Center for Materials and Devices (Japan)," Grant-in-Aid for Scientific Research (Grants No. 25286064, No. 26600111, and No. 16H03881) from MEXT, the Photon Frontier Network Program of MEXT, the Center of Innovation Program from the Japan Science and Technology Agency, JST, and CREST (Grant No. JPMJCR15N1), JST. M. M. and T. M. acknowledge support by the Deutsche Forschungsgemeinschaft (DFG) under Grant No. SFB925/1. We acknowledge the support of the Alexander von Humboldt Foundation (Project Tirinto), the Italian Ministry of Research (Project FIRB No. RBID08CRXK and No. PRIN 2010ERFKXL_006), the bilateral project CNR-JSPS "Ultrafast science with extreme ultraviolet Free Electron Lasers", and funding from the European Union Horizon 2020 research and innovation program under the Marie Sklodowska-Curie Grant Agreement No. 641789 MEDEA (Molecular Electron Dynamics investigated by IntensE Fields and Attosecond Pulses). We thank the machine physicists of FERMI for making this experiment possible by their excellent work in providing high quality FEL light. We thank Vitali Averbukh for helpful discussions.

*ueda@tagen.tohoku.ac.jp
†prince@elettra.trieste.it

[1] L. Meitner, Z. Phys. **9**, 131 (1922).
[2] P. Auger, C.R. Acad. Sci. **177**, 169 (1923).
[3] L. S. Cederbaum, J. Zobeley, and F. Tarantelli, Phys. Rev. Lett. **79**, 4778 (1997).
[4] T. Jahnke *et al.*, Nat. Phys. **6**, 139 (2010).
[5] M. Mucke, M. Braune, S. Barth, M. Förstel, T. Lischke, V. Ulrich, T. Arion, U. Becker, A. Bradshaw, and U. Hergenhahn, Nat. Phys. **6**, 143 (2010).
[6] K. Gokhberg, P. Kolorenc, A. Kuleff, and L. S. Cederbaum, Nature (London) **505**, 661 (2014).
[7] F. Trinter *et al.*, Nature (London) **505**, 664 (2014).
[8] V. Stumpf, K. Gokhberg, and L. S. Cederbaum, Nat. Chem. **8**, 237 (2016).
[9] D. You *et al.*, Nat. Commun. **8**, 14277 (2017).
[10] B. Cooper and V. Averbukh, Phys. Rev. Lett. **111**, 083004 (2013).
[11] P. Ranitovic, X. M. Tong, C. W. Hogle, X. Zhou, Y. Liu, N. Toshima, M. M. Murnane, and H. C. Kapteyn, Phys. Rev. Lett. **106**, 053002 (2011).
[12] X. M. Tong, P. Ranitovic, C. W. Hogle, M. M. Murnane, H. C. Kapteyn, and N. Toshima, Phys. Rev. A **84**, 013405 (2011).
[13] C. W. Hogle, X. M. Tong, L. Martin, M. M. Murnane, H. C. Kapteyn, and P. Ranitovic, Phys. Rev. Lett. **115**, 173004 (2015).
[14] L. S. Cederbaum and J. Zobeley, Chem. Phys. Lett. **307**, 205 (1999).
[15] A. I. Kuleff and L. S. Cederbaum, Chem. Phys. **338**, 320 (2007).
[16] A. I. Kuleff and L. S. Cederbaum, J. Phys. B **47**, 124002 (2014).
[17] F. Calegari *et al.*, Science **346**, 336 (2014).
[18] P. M. Kraus *et al.*, Science **350**, 790 (2015).
[19] K. C. Prince *et al.*, Nat. Photonics **10**, 176 (2016).
[20] M. Gunawardena and D. S. Elliott, Phys. Rev. Lett. **98**, 043001 (2007).
[21] U. Fano, Phys. Rev. A **32**, 617 (1985).
[22] V. Lyamaev *et al.*, J. Phys. B **46**, 164007 (2013).
[23] G. A. Garcia, L. Nahon, and I Powis, Rev. Sci. Instrum. **75**, 4989 (2004).
[24] M. Shapiro and P. Brumer, Rep. Prog. Phys. **66**, 859 (2003).
[25] A. M. Covington, A. Aguilar, I. R. Covington, M. F. Gharaibeh, G. Hinojosa, C. A. Shirley, R. A. Phaneuf, I. Alvarez, C. Cisneros, I. Dominguez-Lopez, M. M. Sant'Anna, A. S. Schlachter, B. M. McLaughlin, and A. Dalgarno, Phys. Rev. A **66**, 062710 (2002).
[26] J. A. R. Samson and W. C. Stolte, J. Electron Spectrosc. Relat. Phenom. **123**, 265 (2002).
[27] M. I. Amusia and L. V. Chernysheva, *Computation of Atomic Processes: A Handbook for the ATOM Programs* (Institute of Physics Pub., Bristol, UK, 1997).
[28] A. V. Korol, J. Phys. B **26**, 4769 (1993).
[29] S. Svensson, B. Eriksson, N. Mårtensson, G. Wendin, and U. Gelius, J. Electron Spectrosc. Relat. Phenom. **47**, 327 (1988).